ChemComm

Small Molecules Reaction Network That Models ROS Dynamic of the Rhizosphere

Journal:	*ChemComm*
Manuscript ID	CC-COM-11-2018-008940.R1
Article Type:	Communication

Journal Name

COMMUNICATION

Small Molecules Reaction Networks That Model ROS Dynamic of the Rhizosphere

Olga Taran,*[a] Vraj Patel [a] and David G. Lynn[a]

Received 00th January 20xx,
Accepted 00th January 20xx

DOI: 10.1039/x0xx00000x

www.rsc.org/

Spontaneous reactions between plant and bacterial redox active metabolites can result in a reaction-diffusion networks that regulate redox gradients and ROS concentrations. Our model system mimics known biological processes observed in plants, including the oxidative burst, travelling waves, and chemical pattern formation. Similar non-enzymatic reactions between natural products may play a role in plant-bacteria interactions, including biofilm and microbiome regulations, and be useful for development of narrow range antibiotics.

A narrow zone of soil along plant root surfaces, known as the rhizosphere, contains bacteria, viruses, fungi and their secondary metabolites.[1] Many of the accumulated compounds have been not only isolated as antibiotics[2] but also functionally implicated in biofilm biogeography,[3] allelopathy,[4] quorum sensing,[5] and specifically in parasitic plant semagenesis.[6] Due to the complexity of biochemical interactions rhizosphere has been called plant's "external metabolome."[7] Chemistry of these complex natural mixtures is poorly understood, despite having clear impact on host-microbiome interactions and even broader biogeochemical cycles.

Many of the isolated metabolites are redox active compounds, such as phenols, quinones, flavins, and phenazines.[8] Reactions of these compounds with molecular oxygen, accumulated along the root surface, often lead to the abiotic formation of reactive oxygen species (ROS), including superoxide radical and hydrogen peroxide.[9] While H_2O_2 can be toxic,[10] low concentrations of reactive oxygen species (ROS) are important for signaling and have been shown to increase the rate of the root growth by loosening lignin polymers found in the cell walls.[11] ROS formation via autoxidation of organic molecules often follows non-linear autocatalytic kinetics that have potential to form complex spatially defined reaction-diffusion networks.[12] While redox cycling dynamics for single molecules in solution have been studied extensively,[13] the interactions in mixtures of redox-cycling molecules and their spatiotemporal behavior remains less-well defined. Here we show that synergetic interaction of two redox active compounds impacts ROS and redox potential dynamic, and may contribute to the spatiotemporal control of several biological processes including the oxidative burst, travelling waves, and chemical pattern formation. We propose a reaction mechanism that can be used to study similar abiotic reactions, which might be widespread in Nature and interfere with wide range of biological processes.

We have focused on two model redox-active compounds (Figure 1a), a plant-derived quinone 2,6-dimehtoxybenzoquinone (DMBQ) and methylene blue (MB), a synthetic proxy for bacterial phenazines.[14] DMBQ and its hydroquinone (H_2DMBQ) are oxidation products of cell wall phenols formed during plant growth, wounding, and wall turnover.[15,16] DMBQ is also a product of wheat germ fermentation with promising anticancer properties.[17] Methylene blue (MB, and its reduced form LMB) is one of the oldest synthetic drugs[18] with similar chemical and biological properties to pyocyanin, an antibiotic produced by the common soil bacteria *Pseudomonas aeruginosa*.[14] ROS formation in the presence of redox active molecules is enabled by redox cycling, a process where oxidized compounds are continuously reduced to maintain the reaction network. Reduction is often performed by plant and bacterial oxidoreductases localized in the plasma membranes.[11] While it is not yet clear whether these enzymes function by one or two electron donor mechanisms,[19] we selected $NaBH_4$ as a hydride donor stand-in for cell wall oxidoreductases.[20,21] In the presence of oxygen, a combination of these three compounds be constitute a minimal model chemistry at the surface of a plant root colonized by bacteria.[38]

The oxidation of both H_2DMBQ and LMB results in color changes that can be followed at 300 and 600 nm, respectively (Figures 1 and S1). The H_2DMBQ/DMBQ redox cycling rate is pH dependent (Figure S2),[22] and while the pH of soils can vary from 5 to 8.5, the root surfaces of monocotyledonous plants maintain a basic pH of 8-9.[23] At pH 8.0 and 8.5, H_2DMBQ oxidation rate has sigmoidal shape that increases with excess DMBQ, indicating autocatalysis (Figure 1b, Figure S2, Schemes S1 and S2, Table S1).

[a] Departments of Chemistry and Biology, Emory University, 1515 Dickey Drive Atlanta, GA, 30322, USA
Electronic Supplementary Information (ESI) available, See DOI: 10.1039/x0xx00000x

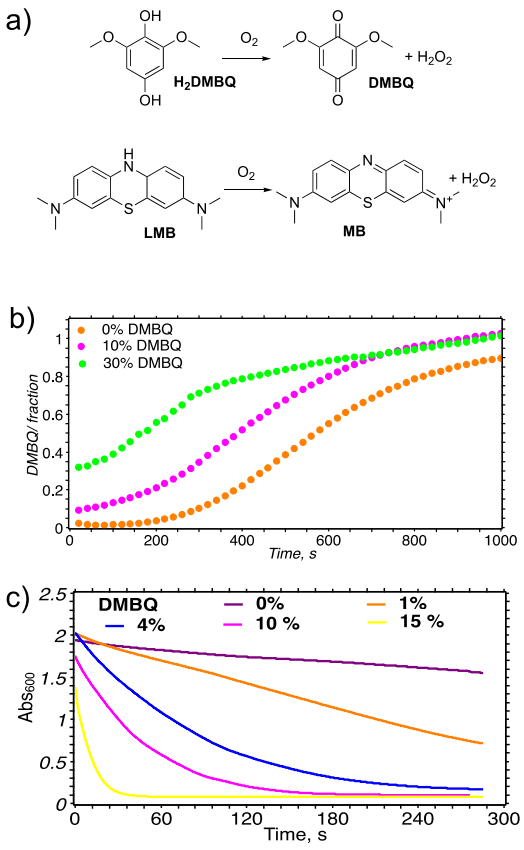

Figure 1. Structure of the reaction network based on two redox active compounds. (a) Redox reactive compounds used in the study. (b) Autocatalytic autoxidation of H_2DMBQ at pH 8.5. (c) DMBQ catalysis of MB reduction with $NaBH_4$.

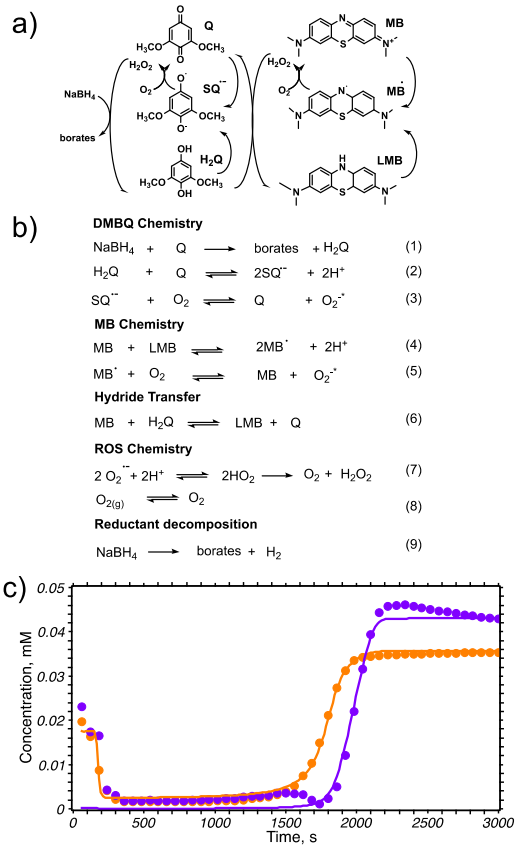

Figure 2. Proposed reaction mechanism: (a) Redox reaction network formed by two molecules in the presence of $NaBH_4$ and O_2; (b) Simplified reaction mechanism; (c) Oxidation reaction and COPASI data fitting for 0.05 mM of DMBQ (orange) and 0.05 mM of MB (purple). Kinetic constants are reported in Table S2.

In biological networks, quinones act as electron shuttles for the more stable heterocyclic compounds.[24] Similarly, in our experiments, MB is not reduced directly by $NaBH_4$ but requires hydride transfer from reduced H_2DMBQ.[25,26] Extremely low concentrations of DMBQ (5×10^{-7} M) are sufficient to significantly alter the redox chemistry of MB in the presence of $NaBH_4$ (Figure 1c). The general reaction mechanism is proposed in Figure 2a and 2b and consists of catalyzed reduction of MB via hydride transfer from hydroquinone and two independent autocatalytic oxidation steps. The full reaction mechanism is presented in Figure 2a. Similar reaction mechanisms have been reported for the reaction of MB and sulfide ion, which is known to show chaotic oscillations, a nonlinear phenomenon.[27] Rate constants for H_2DMBQ and LMB oxidation are compared with previously reported data,[28,29] and the proposed set of kinetic equations (Figure 2b) provide good fits using COPASI[30] software (Figure 2c, Scheme S2, and Table S2).

Here the presence of two redox active compounds, MB and DMBQ, results in synchronizing the oxidation step. The network apparently exists in two states, a "fully reduced" in the presence of excess reducing agent over dissolved oxygen, and "fully oxidized", when oxygen concentration (0.220 mM in saturated solution) is higher than the $NaBH_4$ concentration. The transition between these states can be further controlled using different concentrations of $NaBH_4$ (Figure S5).

Autoxidation of the reduced compounds by molecular oxygen leads to oxygen consumption and the formation of H_2O_2. In a single component mixture, the amount of oxygen converted to H_2O_2 is proportional to the concentration of the redox cycling compound, however the addition of a second redox-active component drastically changes the reactive oxygen species (ROS) dynamics in the network (Figure 3). While excess $NaBH_4$ slows oxygen consumption in the presence of DMBQ, the addition of MB leads to fast oxygen consumption and formation of an anoxic solution (Figure 3a). Due to a low reduction rate of MB by $NABH_4$, redox cycling between LMB/MB and the associated H_2O_2 production are very low. Addition of even small amount of DMBQ to MB (1% or 500 nM DMBQ) increases the rate of production of H_2O_2 by almost an order of magnitude. Further increase of DMBQ concentration results in conversion of all available oxygen to hydrogen peroxide (Figure 3a, b). As shown in the Figure 3c, COPASI simulation based on the reaction mechanism proposed on Figure 2b explains this observation. In a single component system, oxidation of H_2DMBQ in the presence of $NaBH_4$ is suppressed due to constant reduction of autocatalytic DMBQ, and hydrogen peroxide production begins only after all $NaBH_4$ is removed from the system. In the multi-component system, oxidation of LMB is independent of the concentration of reducing agent, a steady state concentration of DMBQ is maintained due to H_2DMBQ oxidation by MB, and both autoxidation reactions are active, leading to fast conversion of oxygen to H_2O_2 (Figure 3c).

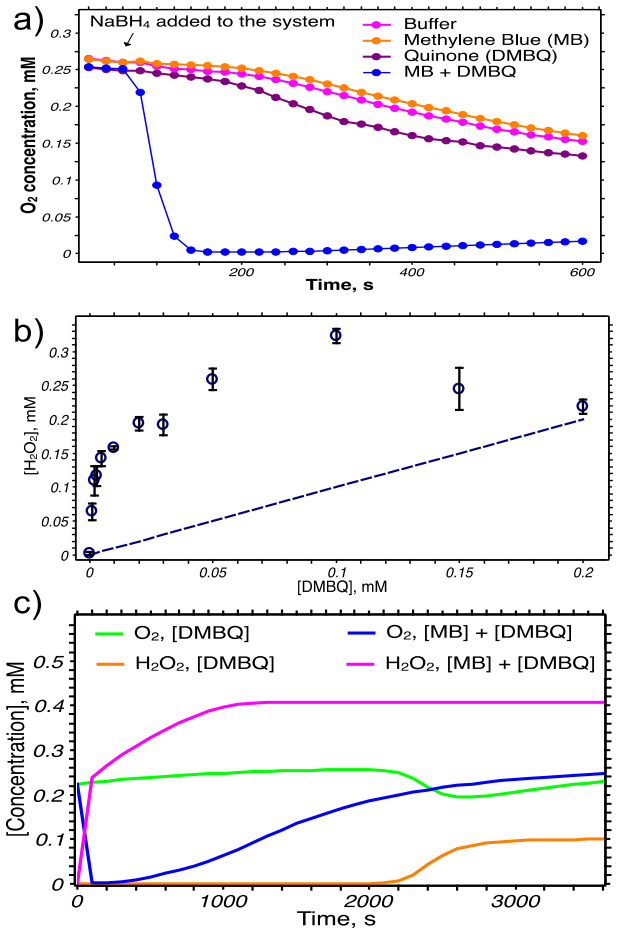

Figure 3. ROS dynamics in the MB/DMBQ system. (a) Oxygen consumption after 1 mM of $NaBH_4$ is added to the system at 60 s (marked with arrow). (b) H_2O_2 production in the presence of 0.05 mM MB, 1 mM $NaBH_4$, and variable concentrations of DMBQ measured 1h after the reaction start time. The dashed line corresponds to H_2O_2 production expected with DMBQ alone. (c) COPASI simulation of O_2 consumption and H_2O_2 production with DMBQ alone and in the presence of MB and DMBQ.

Similar fast ROS production occurs at a plant's wound site. There reduced phenolic compounds from the cell come in contact with cell wall oxidoreductases and molecular oxygen to create the "oxidative burst," enabling the extremely rapid generation of an anoxic environment, production of high concentrations of H_2O_2 for the sterilization of the wound, and the initiation of radical lignin polymerization ensuring wound repair.[31]

Many processes in the rhizosphere seem to be timed and coordinated over millimeter to centimeter distances that cannot be regulated by simple diffusion of signaling molecules.[32] We found that the reduction of MB and DMBQ initiated by a small sample of solid $NaBH_4$ results in fast propagation of an anoxic wave front in 1% agarose gel (Figure 4a and SI LapseClip1). The reducing front propagates *via* fast hydride transfer equilibrium between quinone and MB, and autocatalytic removal of oxygen from the solution (Figure S8), which leads to the formation of a sharp diffusion front. There is no color change in the absence of DMBQ (Figure S7), due to the low rate of uncatalyzed reduction of MB by $NaBH_4$. The anoxic clear area propagates linearly over 1 h and is arrested when all the reducing agent is consumed. If a thin layer of the gel is open to the air, the initial fast propagation of the anoxic layer stops after several minutes and the gel is rapidly reoxidized. A similar reaction mechanism may help to explain the spatial localization of host-specific germination in *Striga asiatica* where a hydroquinone germination stimulant remains reduced along the growing sorghum root for days despite the oxidizing environment,[33] and might be relevant to well-known role of quinones as quorum-quenching agents.[34]

Finally, a dynamic reaction-diffusion system is formed during the oxidation of DMBQ and MB in a thin layer of liquid on the surface of a Petri dish exposed to air. Well-defined redox patterns with two distinct modes of action are observed (SI LapseClip2 and LapseClip3, Figure 4c). When both oxygen and $NaBH_4$ are present in solution, fast propagating pulsating rings radiate across the plate. Raising the DMBQ concentration leads to an increase in the size and number of rings. When starting from anoxic mixtures, slow reaction between uncolored reduced solution and atmospheric oxygen produces stable patterns of regularly spaced dark blue lines. Similar phenomena have been previously reported for the reaction of methylene blue and peroxidase enzymes (modified Blue Bottle Experiment) and attributed to the action of reaction-driven Rayleigh–Bénard convection.[35] To confirm that the mechanism is due to hydrodynamic phenomena, we have shown that there is no pattern formation in 1% agarose gel where water dynamic is arrested. Additionally, the spacing between lines is controlled by the thickness of the liquid layer (Figure S9) and thus by the size of the convection cell. The pattern progresses over time from thin blue lines, to thicker lines with changing color, to white lines on a blue background, to unevenly shaped concentric dark blue circles on light blue background, and finally to a uniformly blue solution. The lifetimes of the patterns are controlled by pH, which impacts the stability of $NaBH_4$. At pH 8.5, patterns form in the presence of 0.05 mM MB, 0.05 mM DMBQ and 2 mM $NaBH_4$ over 30 minutes, but at pH 8.0, the window is reduced to 15 minutes. Visually these patterns resemble the structure of some biofilms[36] but it remains to be seen if similar reactions play a role in biofilm establishment and spatial organization.

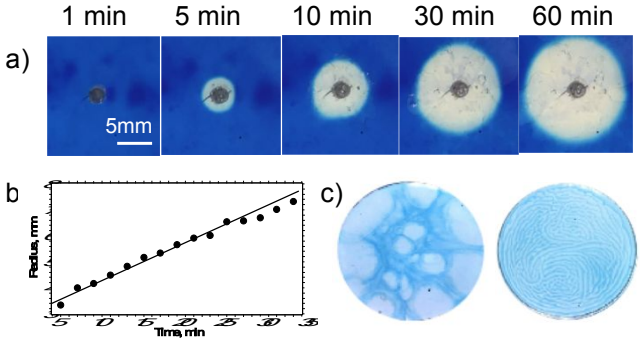

Figure 4. Reaction-diffusion phenomena in the MB/DMBQ system. (a) Time-dependent propagation of the reducing front (colorless) in DMBQ: MB mixture (blue) in a thin layer of the agarose gel. (b) Linear propagation of the travelling reduced front over time. (c) Pattern formation in a thin layer of liquid. Left: pulsating rings (excess of oxygen); right: blue lines on white background observed when starting from anoxic solution.

The plant cell wall contains a diverse range of phenolic acids as possible quinone precursors. To understand how this spectrum of quinones might participate in the reaction-diffusion networks, we evaluated both natural and synthetic quinones as catalysts for MB reduction by $NaBH_4$ (Table S3). In general, naturally occurring methoxy- and hydroxyquinones are effective catalysts, while the less biologically abundant unsubstituted hydroquinone is not effective. Quinone activity is also regulated by pH. Methoxyquinones are reactive at mildly basic pH (7.5-9), while hydroxyquinones and some naphthoquinones show higher activity in more acidic environments (pH 6-7). Soil and root surface pH varies from plant to plant and pH regulation might contribute to the specificity of these redox processes in the rhizosphere.

We have shown how the interaction between two redox active molecules in a thermodynamically open system can lead to spatial and temporal organization of ROS and redox gradients resembling those found in the rhizosphere, while diffusion of a signalling molecules alone cannot explain spatial organization patterns observed in microbiomes and biofilms. Achieving large-scale spatiotemporal resolution through regulated reaction-diffusion networks could provide a framework for understanding redox processes in Nature. The area of Systems Chemistry[37] can help in further development of kinetic models of multicomponent systems, necessary for the characterization of environmental processes and interaction within complex biological communities.

Conflicts of interest

There are no conflicts to declare.

Notes and references

1 D. Bulgarelli, K. Schlaeppi, S. Spaepen, E. V. L. van Themaat and P. Schulze-Lefert, *Annu. Rev. Plant Biol.*, 2013, **64**, 807–838.
2 L. L. Ling, T. Schneider, A. J. Peoples, A. L. Spoering, I. Engels, B. P. Conlon, A. Mueller, T. F. Schaberle, D. E. Hughes, S. Epstein, M. Jones, L. Lazarides, V. A. Steadman, D. R. Cohen, C. R. Felix, K. A. Fetterman, W. P. Millett, A. G. Nitti, A. M. Zullo, C. Chen and K. Lewis, *Nature*, 2015, **517**, 455–459.
3 A. Stacy, J. Everett, P. Jorth, U. Trivedi, K. P. Rumbaugh and M. Whiteley, *Proc. Natl. Acad. Sci.* , 2014, **111**, 7819–7824.
4 A. Tomilov, N. Tomilova, D. H. Shin, D. Jamison, M. Torres, R. Reagan, H. Mcgray, T. Horning, R. Truong, A. J. Nava and J. I. Yoder, in *Chemical Ecology: from Gene to Ecosystem*, 2006, pp. 55–69.
5 A. W. Fuller, P. Young, B. D. Pierce, J. Kitson-Finuff, P. Jain, K. Schneider, S. Lazar, O. Taran, A. G. Palmer and D. G. Lynn, *PLoS One*, , DOI:10.1371/journal.pone.0182655.
6 W. J. Keyes, A. G. Palmer, W. K. Erbil, J. V Taylor, R. P. Apkarian, E. R. Weeks and D. G. Lynn, *Plant J.*, 2007, **51**, 707–716.
7 N. R. Glasser, S. H. Saunders and D. K. Newman, *Annu. Rev. Microbiol.*, 2017, **71**, 731–751.
8 J. Sasse, E. Martinoia and T. Northen, *Trends Plant Sci.*, 2018, **23**, 25–41.
9 D. Uteau, S. Hafner, S. K. Pagenkemper, S. Peth, G. L. B. Wiesenberg, Y. Kuzyakov and R. Horn, *J. Plant Nutr. Soil Sci.*, 2015, **178**, 278–287.
10 J. L. Bolton, M. A. Trush, T. M. Penning, G. Dryhurst and T. J. Monks, *Chem. Res. Toxicol.*, 2000, **13**, 135–160.
11 M. Potocký, M. A. Jones, R. Bezvoda, N. Smirnoff, V. Žárský and V. Zárský, *New Phytol.*, 2007, **174**, 742–751.
12 I. Epstein and J. Pojman, *An Introduction to Nonlinear Chemical Dynamics: Oscillations, Waves, Patterns, and Chaos*, Oxford University Press, New York, 1998.
13 Y. Song and G. R. Buettner, *Free Radic. Biol. Med.*, 2011, **49**, 919–962.
14 D. M. Kasozi, S. Gromer, H. Adler, K. Zocher, S. Rahlfs, S. Wittlin, K. Fritz-Wolf, R. H. Schirmer and K. Becker, *Redox Rep.*, 2011, **16**, 154–165.
15 C. Mayland and D. G. Lynn, in *Allelochemicals: Role in Agriculture and Forestry*, 1987, vol. 330, pp. 49–551.
16 C. Songkui, W. Syogo, T. Yuki, T. Yuri, S. S. B., T. Toshiyuki, U. Toshiaki, S. Ken and Y. Satoko, *New Phytol.*, 2018, **218**, 710–723.
17 E. M. Koh, E. K. Lee, J. Song, S. J. Kim, C. H. Song, Y. Seo, C. H. Chae and K. J. Jung, *J. Food Biochem.*, 2018, **0**, e12688.
18 J. C. Y. Lo, M. A. Darracq and R. F. Clark, *J. Emerg. Med.*, 2017, **46**, 670–679.
19 R. L. Wrobel, M. Matvienko and J. I. Yoder, *Plant Physiol. Biochem.*, 2002, **40**, 265–272.
20 J. Foreman, V. Demidchik, J. H. F. Bothwell, P. Mylona, H. Miedema, M. A. Torres, P. Linstead, S. Costa, C. Brownlee, J. D. G. Jones, J. M. Davies and L. Dolan, *Nature*, 2003, **422**, 442–446.
21 M. V. C. Nguyen, B. Lardy, F. Rousset, F. Hazane-Puch, L. Zhang, C. Trocmé, L. Serrander, K. H. Krause and F. Morel, *Biochem. Pharmacol.*, 2013, **85**, 1644–1654.
22 V. A. Roginsky, G. Bruchelt and H. B. Stegmann, *Biochem.*, 1998, **63**, 200–206.
23 S. Blossfeld, C. M. Schreiber, G. Liebsch, A. J. Kuhn and P. Hinsinger, *Ann. Bot.*, 2013, **112**, 267–276.
24 J. Dou, P. Lin, B. Y. Kuang and J. Z. Yu, *Environ. Sci. Technol.*, 2015, **49**, 6457–6465.
25 M. G. Roberts, D. Ostovic and M. M. Kreevoy, *Faraday DIscuss. Chem. Soc.*, 1982, **74**, 257–265.
26 Y. Liu, S. Yamamoto, Y. Fujiyama and Y. Sueishi, *Phys. Chem. Chem. Phys.*, 2000, **2**, 2367–2371.
27 Y.-X. Zhang and R. J. Field, *J. Phys. Chem.*, 1991, **95**, 723–727.
28 V. A. Roginsky, L. M. Pisarenko and C. Michel, *J. Chem. Soc., Perkin Trans.*, 1999, 871–876.
29 A. Katafias and S. Koter, *Pol. J. Chem.*, 2009, **Vol. 83**, **n**, 1139–1146.
30 S. Hoops, S. Sahle, R. Gauges, C. Lee, J. Pahle, N. Simus, M. Singhal, L. Xu, P. Mendes and U. Kummer, *Bioinformatics*, 2006, **22**, 3067–3074.
31 R. Tenhaken, A. Levine, L. F. Brisson, R. A. Dixon and C. Lamb, *Proc Natl Acad Sci U S A*, 1995, **92**, 4158–4163.
32 S. Soh, M. Byrska, K. Kandere-Grzybowska and B. A. Grzybowski, *Angew. Chem. Int. Ed. Engl.*, 2010, **49**, 4170–4198.
33 M. Chang, D. H. Netzly, L. G. Butler and D. G. Lynn, *J. Am. Chem. Soc.*, 1986, **108**, 7858–7860.
34 V. C. Kalia, *Biotechnol. Adv.*, 2013, **31**, 224–245.
35 Y. Zhang, S. Tsitkov and H. Hess, *Nat. Catal.*, 2018, **1**, 276–281.
36 C. Okegbe, B. L. Fields, S. J. Cole, C. Beierschmitt, C. J. Morgan, A. Price-Whelan, R. C. Stewart, V. T. Lee and L. E. P. Dietrich, *Proc. Natl. Acad. Sci.*, 2017, 201700264.
37 G. Ashkenasy, T. M. Hermans, S. Otto and A. F. Taylor, *Chem. Soc. Rev.*, 2017, **46**, 2543–2554.
38. Please refer to Supporting Information for full description of experimental procedures.

Molecules released by plants and bacteria form complex abiotic reaction diffusion network that might regulate the ROS dynamics along the roots of the plants